ЖУРНАЛ ФІЗИЧНИХ ДОСЛІДЖЕНЬ
т. 3, № 4 (1999) с. 431–436

JOURNAL OF PHYSICAL STUDIES
v. 3, No. 4 (1999) p. 431–436

# FINAL–STATE INTERACTION AND QUASI–FREE SCATTERING IN THE FOUR–BODY $d+d$ REACTION AT 46.7 MeV

B. Struzhko
*Institute for Nuclear Research of the National Academy of Science of Ukraine,*
*47 Nauky Pr., Kyiv, UA–03028, Ukraine*

(Received May 11, 1999; received in final form July 17, 1999)

Two–dimensional proton–proton ($pp$) and proton–proton–neutron ($ppn$ ) coincidence spectra from $d+d \longrightarrow p+p+n+n$ four–body break–up are calculated. Quasifree scattering (QFS) of protons in the plane wave impulse approximation and final state interaction of neutron–proton pairs in the Watson–Migdal approximation are taken into account. Calculations are in reasonable agreement with the experimental data obtained at the deuteron beam energy $E_0 = 46.7$ MeV, proton angles in the lab. system $\vartheta_1 = \vartheta_2 = 38.75°$, $\varphi_1 - \varphi_2 = 180°$ and the neutron one $\vartheta_n = 0°$ which are the $pp$ QFS kinematic conditions. Contribution from the sequential $d+d \longrightarrow d^* + d^* \longrightarrow p+p+n+n$ process is found to prevail in the double pp coincidence spectrum while only about the fourth part of all events are from $pp$ QFS. This conclusion is supported by a direct comparison of the model and measured ratios of triple $ppn$ coincidence events to the double pp ones.

**Key words:** deuteron, four–body, break–up, 46.7 MeV, quasi–free scattering, final–state interaction.

PACS number(s): 25.10.+s, 25.45.–z, 25.70.Bc

## I. INTRODUCTION

At present four–nucleon (4N) systems become a subject of growing interest. With improved calculations, they can be used to probe the nucleon–nucleon (NN) interaction, in particular many–nucleon and off–shell components, or on–shell P interaction. $4N$ systems are the simplest ones which can be used for investigating neutron–neutron ($nn$) scattering with charge particle beams. Some years ago H. Kumpf proposed to use quasifree scattering (QFS) of neutrons in $d+d$ collisions for measuring $nn$ scattering parameters: the scattering length $a_{nn}$ and (mainly) the effective range $r_{nn}$ [1]. In this process the neutron from the incident deuteron scatters from the neutron in the target deuteron according to the binary kinematic relations while both of protons remain with their initial momenta. For this reason it is referred to as a double spectator process (DSP) [2] or two spectator quasifree scattering (TSQFS) [3]. I do not know any investigation of that kind by now. There are some publications about search of the proton–proton ($pp$) QFS in the mirror $^2$H$(d,pp)$ reaction [2–5]. Naturally, such experiments allow to estimate main characteristics of the $^2$H$(d,nn)$ reaction, such as cross sections and background of nonQFS contributions to spectra. Two–dimensional $pp$ coincidence spectra were measured at beam energies $E_0 = 34.7$ MeV [3], 50 MeV [4], 80 MeV [2] and 108 MeV [5]. Besides deuteron–deuteron ($dd$) QFS for the $^3$He($^3$He$,dd$) reaction was investigated at $E_0 = 50$ and 78 MeV [3] and proton–neutron ($pn$) coincidences were also obtained at $E_0 = 108$ MeV [5]. Shapes of measured spectra were in satisfactory agreement with plane wave Born approximation calculations [2] or plain wave impulse approximation (PWIA) ones [3,5], but the ratio of cross sections $N = \dfrac{\text{experiment}}{\text{theory(PWIA)}}$ is found to be larger for the $^2$H$(d,pp)$ reaction, than for the $^3$He($^3$He$,dd$) one at equal energies [3].

On the other hand, a competing process could contribute to the $pp$ coincidence spectra viz. the $^2$H$(d,d^*)d^*$ reaction or the so–called double final state interaction (DFSI) [2] because the kinematic condition of it is very close to that of the TSQFS. Simple kinematic calculations show, that at beam energy 50 MeV symmetric angles and energies of protons emitted are 39 degrees and 10.3 MeV in the QFS and 42 degrees and 11.4 MeV in the DFSI process respectively. Straight calculations also show that angular and energy distributions of protons are similar in these two processes [6,7]. The $nn$ and $pp$ FSI in the $^2$H$(d,pp)$ reaction were found out in experiments [8,9] and the DFSI process was identified in complete experiment [10].

Recently double $pp$ and triple $ppn$ coincidence spectra were measured in conditions of $pp$ TSQFS at beam energy $E_0 = 46.7$ MeV [11]. This is an only observation of the DSP in a complete experiment so far. The existence of the TSQFS in the $^2$H$(d,pp)$ reaction thus was proved but contributions of different processes to spectra could not be determined because of a very approximate model used. Now a new attempt is undertaken to define more precise contributions of various mechanisms by simulating $pp$ and $ppn$ coincidence spectra with account of the $np$ FSI and $pp$ QFS and comparing them to the experimental data [11]. PWIA and Watson–Migdal models are used in the calculations and effects of the target and detector dimensions and resolutions are taken into account as well.

## II. EXPERIMENTAL DATA

A TiD target was bombarded with deuterons whose energy at the target centre was 46.7 MeV. Charged particles were detected by two $\Delta E - E$ counter telescopes placed symmetrically to the beam. Angles of detected particles $\vartheta_1 = \vartheta_2 = 38.75°$ correspond to the pp DSP condition. Neutrons emitted along the beam direction were detected using a plastic scintillator (10 cm wide $\times$10 cm high $\times$ 20 cm thick). The distance between the target and the centre of the neutron detector was 1.3 m. Other experimental details can be found in Ref. [11].

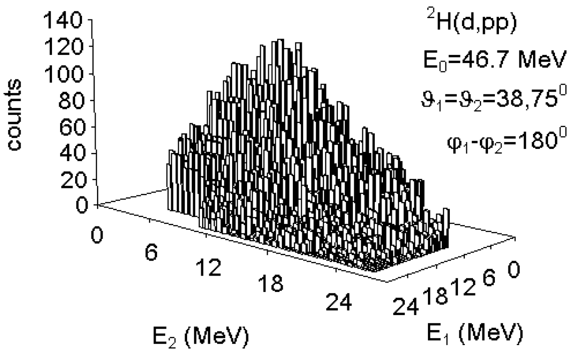


Fig. 1. Two–dimensional $pp$ coincidence spectrum. Beam energy $E_0 = 46.7$ MeV, angles of protons $\vartheta_1 = \vartheta_2 = 38.75°$, $\varphi_1 - \varphi_2 = 180°$.

Two–dimensional $pp$ coincidence spectrum obtained is shown in Fig. 1. Here it is depicted for protons of 4.5 MeV and upwards. A random coincidence background and effects of $^1$H$(d,pp)$ breakup from the light hydrogen contamination in the target have been eliminated. Actually the amount of these impurities was much less than 1 per cent but that was enough to deform a spectrum at proton energies in the vicinity of 6 MeV because of a huge difference in the $^1$H$(d,pp)$ and $^2$H$(d,pp)$ cross sections. More than 30 thousand true $pp$ coincidence events $N_{pp}$ have been collected for this spectrum. Besides more than one hundred triple $ppn$ coincidence events $N_{ppn}$ have been recorded in complete experiment. The ratio $N_{ppn}/N_{pp} = 0.0061 \pm\ 0.0007$ has been obtained.

## III. THE MODEL

The differential cross sections of the four–particle $^2$H$(d,pp)$ reaction are calculated by using the prescription [6,12]:

$$\frac{d^4\sigma(E_1,E_2,\vartheta_1,\vartheta_2,\varphi_1,\varphi_2)}{d\Omega_1 d\Omega_2 dE_1 dE_2} = \frac{(2\pi)^4}{v}\int \rho|F|^2 sin\vartheta d\vartheta d\varphi, \tag{1}$$

where $E_1, E_2$ are energies of protons, $v = p_0/2m$ is a velocity of the deuteron in the beam, $\mathbf{p}_0$ is a deuteron momentum, $m$ is the nucleon mass, $\rho$ is a phase space factor [12], $\vartheta$ and $\varphi$ are angles of a relative neutron–neutron momentum $\mathbf{k}_{nn}$, $F$ is a transition matrix element. In calculations of the double coincidence spectrum $N_{pp}(E_1,E_2)$ an integration domain covers all possible directions $\mathbf{k}_{nn}$ (i.e. within $4\pi$), and for triple coincidence $N_{ppn}(E_1,E_2)$ it is defined by a solid angle of the neutron detector. Matrix element is approximated as a sum:

$$|F|^2 = c_1|F_{QF}|^2 + c_2|F_S|^2 + c_3|F_T|^2 \tag{2}$$

where $F_{QF}$ is the $pp$ QFS amplitude and $F_S$ and $F_T$ are the FSI amplitudes for the $^1S_0$ and $^3S_1$ $np$ states respectively, $c_1 - c_3$ are free parameters. Here interference effects between QFS and FSI amplitudes can be neglected because of completely different angular and energy distributions of neutrons. QFS amplitude is evaluated using PWIA [3,13]:

$$|F_{QF}|^2 = \left|\psi\left(\frac{\mathbf{p}_{pp}}{2} - \mathbf{k}_{nn}\right)\right|^2 \left|\psi\left(\mathbf{k}_{nn} - \frac{\mathbf{p}_{nn}}{2}\right)\right|^2 \frac{d\sigma_{pp}(\mathbf{k}_{pp})}{d\Omega}$$

with $\mathbf{p}_{pp} = \mathbf{p}_1 + \mathbf{p}_2$ and $\mathbf{p}_{nn} = \mathbf{p}_0 - \mathbf{p}_{pp}$, where $\mathbf{p}_1$, $\mathbf{p}_2$ are momenta of protons in the lab. system,

$$k_{nn} = \sqrt{mE_{nn}}, \qquad E_{nn} = E_0 + Q - E_1 - E_2 - \frac{p_{nn}^2}{4m},$$

$$Q = -4.449 \text{ MeV}, \quad \mathbf{k}_{pp} = \frac{(\mathbf{p}_1 - \mathbf{p}_2)}{2},$$

$$\psi(\mathbf{k}) = (2\pi)^{-3/2}\int \psi(\mathbf{r})e^{-i\mathbf{kr}}d^3\mathbf{r}$$

is a Fourier component of the deuteron wave function. It is taken in the Hulthen form:

$$\psi(r) = \sqrt{\frac{\alpha\beta(\alpha+\beta)}{2\pi}}\frac{e^{-\alpha r} - e^{-\beta r}}{(\alpha-\beta)r},$$

$h^2\alpha^2 = mE_\alpha$, $E_\alpha = 2.2245$ MeV, $h^2\beta^2 = mE_\beta$, $E_\beta =$ 59.8 MeV. Calculations are carried out in the simple impulse approximation (SIA) with

$$|\psi(k)|^2 = \frac{\alpha\beta(\alpha+\beta)^3}{\pi^2(\alpha^2+k^2)^2(\beta^2+k^2)^2}$$

and in the modified one (MIA) [14] with

$$|\psi(k)|^2 = \frac{\alpha\beta(\alpha+\beta)}{\pi^2(\alpha-\beta)^2}\left|e^{-\alpha R}\frac{\frac{\alpha}{k}\sin kR + \cos kR}{\alpha^2+k^2} + e^{-\beta R}\frac{\frac{\beta}{k}\sin kR + \cos kR}{\beta^2+k^2}\right|^2$$

and the chosen cutoff parameter of the deuteron wave function $R = 4.6\ fm$. Keeping in mind that $k_{pp}$ is rather moderate for S wave interaction to be used and rather high for Coulomb terms to be neglected the cross section of proton–proton elastic scattering is used in the form [15]:

$$\frac{d\sigma_{pp}(k)}{d\Omega} = \frac{1}{k^2 + (-\frac{1}{a_{pp}} + \frac{1}{2} r_{pp} k^2)^2},$$

with $a_{pp} = -7.813\ fm$ and $r_{pp} = 2.78\ fm$ [16].

$F_S$ and $F_T$ terms in (2) are calculated by using the Watson–Migdal approximation:

$$|F_S|^2 = |F_{1S}|^2 \, |F_{2S}|^2 ,$$

where $F_{1S}$ and $F_{2S}$ correspond to neutron–proton pairs emitted on the left and to the right of the beam respectively:

$$F_{1(2)S} = \frac{r_{np}(k^2 + \kappa^2)}{2(-\frac{1}{a_{np}} + \frac{1}{2} r_{np} k^2 - ik)},$$

$\kappa = \frac{1}{r_{np}}(1 + \sqrt{1 - \frac{2r_{np}}{a_{np}}})$, $hk = \sqrt{mE_{np}}$. The expressions for $F_T$ are similar. Parameters $a_{np}$ and $r_{np}$ are equal $-23.748\ fm$ and $2.75\ fm$ for the $^1S_0$ np state and 5.424 fm and $1.759\ fm$ for the $^3S_1$ one [16].

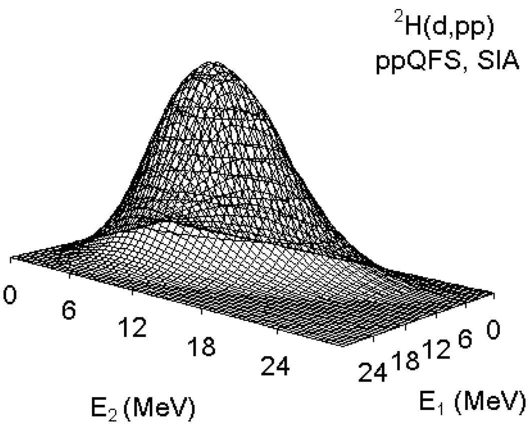


Fig. 2. Simulated *pp* coincidence spectrum for the $^2$H$(d, pp)$ reaction. SIA.

Calculations are carried out with the Monte–Carlo method, in this case the angles $\vartheta$, $\varphi$ and the position of particles on the target and detector slits are taken as random numbers. The results of Refs. [3] (table 1) and [6] (Fig. 1) were used for checking the computer code.

## IV. RESULTS

Simulated *pp* coincidence spectrum is shown in Fig. 2. Only the first term in the sum (2) is taken into acount and SIA is used. Cross sections on the cut along the $E_1 = E_2$ line are shown in Fig. 3 (a solid line). It is easy to see that the theoretical curve is a bit shifted from experimental points to lower energies. So there may be something else in the spectrum, that is not taken into account in calculations. Calculated cross sections are multiplied by the factor $c_N = 0.2$. It is four times higher, than the value 0.049, obtained for *dd* QFS in the $^3$He($^3$He, $dd$)$2p$ reaction at the beam energy of 50 MeV [3] where *pd* FSI effects are not essential at all. SIA and MIA calculations without the target and detector dimensions and resolutions taken into account are shown as dashed and dotted lines. The $c_N$ factors are 0.2 and 1.0 respectively as well.

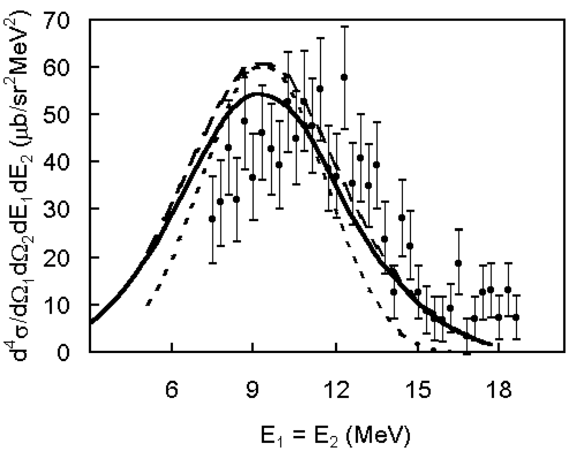


Fig. 3. Simulated cross–sections for *pp* QFS (SIA) and the data along the $E_1 = E_2$ line. Dashed and dotted lines are the SIA and MIA calculations for dot geometry and ideal resolution.

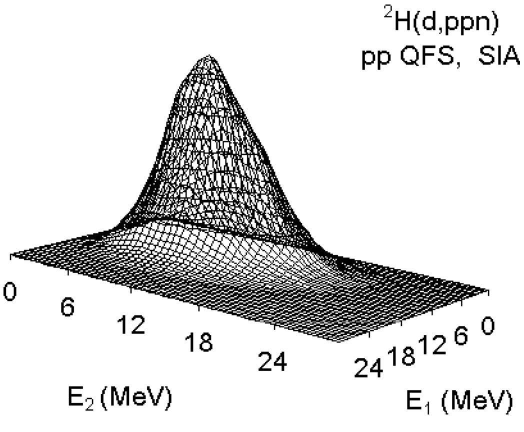


Fig. 4. Simulated *ppn* coincidence spectrum for the $^2$H$(d, ppn)$ reaction. SIA.

Simulated two–dimensional $ppn$ coincidence spectrum is depicted in Fig. 4. It is difficult to compare it to the experimental spectrum because of poor statistics in the last one. On the other hand, total number of $ppn$ coincidence events can be used for the estimation of the QFS effect in the $pp$ coincidence spectrum. Though of SIA does not reproduce absolute values of cross sections at our energies [17] their relative dependence on spectator momenta are consistent with experimental ones [13,15]. Angular distribution of neutrons–'spectators' from $^2$H$(d, ppn)$ reaction is strongly directed forward.The function $\frac{dN}{d(\cos\vartheta)} \sim \frac{1}{0.0019+\sin^3\vartheta}$ is a good approximation for a simulated angular distribution of neutrons at the angles $\vartheta_n < 20°$. Likewise the Gaussian function $\frac{dN}{dE_n} \sim \exp\{-\ln 2\frac{(E_0-En)^2}{\mathrm{H}^2}\}$ with $E_0 = 23.4$ MeV and $H = 5.5$ MeV is a good approximation for a simulated neutron spectrum at $\vartheta_n = 0°$. The average efficiency $\eta$ of the neutron detector is calculated with the adapted Stanton code [18]. The ratio $\frac{\eta N_{ppn}}{N_{pp}} = 0.026$ quadruples the experimental value. This result can be interpreted assuming that the QFS contribution to the $pp$ coincidence spectrum on Fig. 1 really exists but amounts only to about a quarter of all the events.

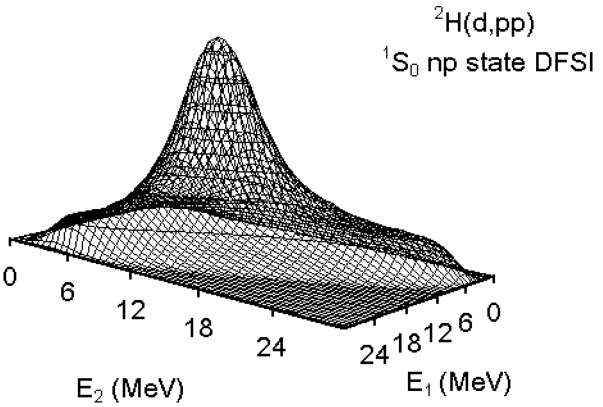


Fig. 5. Simulated $pp$ coincidence spectrum. The Watson–Migdal approximation for $^1S_0$ $np$ FSI.

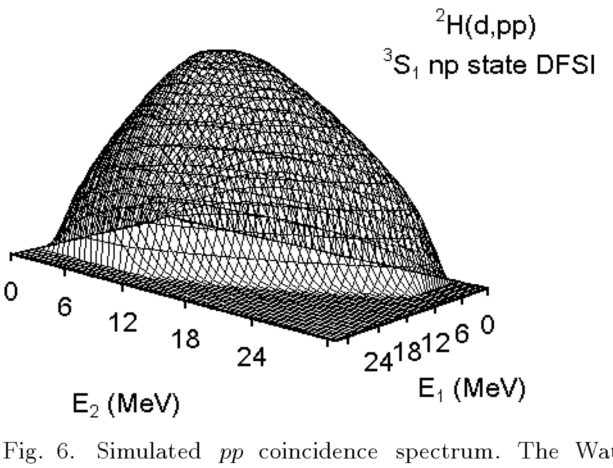


Fig. 6. Simulated $pp$ coincidence spectrum. The Watson–Migdal approximation for $^3S_1$ $np$ FSI.

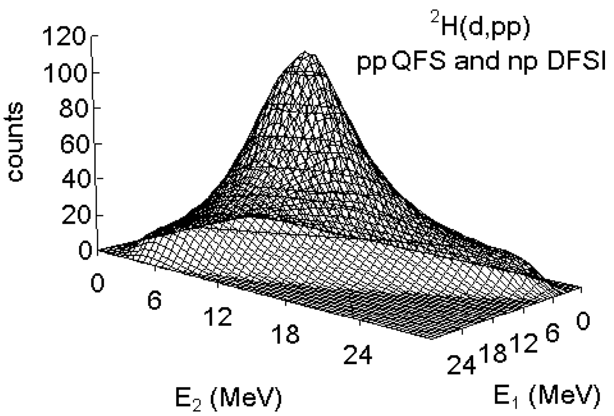


Fig. 7. Simulated $pp$ coincidence spectrum with all three amplitudes in the sum (2) taken into account. Fitting with the least squares method.

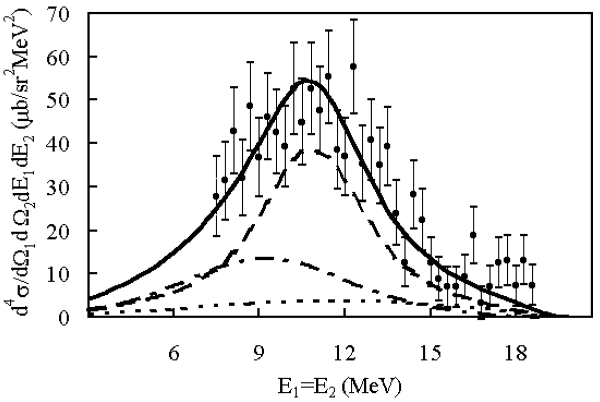


Fig. 8. Cuts of surfaces in Fig. 1 and 9 along the $E_1 = E_2$ line. Dashed–dotted, dashed and dotted lines are for the $pp$ QFS (SIA), $^1S_0$ and $^3S_1$ $np$ FSI respectively and the solid line is their total contribution.

The contribution from QFS to spectra can be estimated differently by a direct fitting of a simulated $pp$ coincidence spectrum to the experimental one. The spectra calculated for $^1S_0$ and $^3S_1$ $np$ FSI are shown in Fig. 5 and 6. One can see that Fig. 2 and 5 are really similar so in fitting procedure as many experimental points must be used as possible to achieve the unambiguous result. Strictly speaking $nn$ FSI should be also taken into account but it was not found out in fitting so the effect of only three terms in the sum (2) is discussed. Such a simulated spectrum with all the three amplitudes in the sum (2) taken into account is given in Fig. 7. The factors $c_1 - c_3$ are free parameters. The fitting area in a plane $E_1 - E_2$ is bounded with thresholds 7.8 MeV $\leq E_1, E_2$ and four–body limit of the $d+d \rightarrow p+p+n+n$ reaction with the $Q$–value being equal -4.449 MeV and contains $m = 2694$ elements of an experimental matrix $N_{ijex}$ with the errors $\Delta N_{ijex}$ and simulated one $N_{ijsim}$. The value $\chi^2 = \frac{1}{m-3}\sum\frac{(N_{ijex}-N_{ijsim})^2}{\Delta N_{ijex}^2}$ has appeared to be equal 1.51, and the ratio of contributions from the various terms in (2) on this area is

$(0.20 \pm 0.04)$ : $(0.65 \pm 0.07)$ : $(0.15 \pm 0.03)$ in agreement with the experimental value $\frac{N_{ppn}}{N_{pp}}$. Recalculated on the entire kinematically allowed area this ratio becomes $(0.24 \pm 0.04)$ : $(0.61 \pm 0.06)$ : $(0.15 \pm 0.03)$. Calculated cross sections and experimental data on the cut along the $E_1 = E_2$ line are shown in Fig. 8. The dash–dotted, dashed and dotted lines show the QFS component and the FSI ones for $^1S_0$ and $^3S_1$ $np$ states respectively. The ratio of the corresponding contributions to the total curve in a the range of [0–23.4] MeV is $(0.28 \pm 0.05) : (0.60 \pm 0.06) : (0.12 \pm 0.02)$.

A reasonable variation of the fitting area does not change the results essentially. For example, on the fitting area bounded with the thresholds 7.8 MeV $\leq E_1, E_2$ and the four–body limit with $Q = -5.449$ MeV ($m =$ 2405), $\chi^2 = 1.44$ and the ratio becomes $(0.22 \pm 0.03)$ : $(0.58 \pm 0.05)$ : $(0.20 \pm 0.03)$ which is transformed into $(0.26 \pm 0.04) : (0.53 \pm 0.05) : (0.21 \pm 0.03)$ at the entire allowed area.

## V. SUMMARY

Experimental cross sections of the four–body $d + d$ break–up and their parametrization in a simple form are presented which will facilitate a comparison of the data with rigorous theoretical calculations when they are possible. The two–dimensional pp coincidence spectrum can be reasonably fitted by an incoherent sum of the DSP and DFSI contributions. The results of fitting confirm that in an incomplete $^2$H$(d, pp)$ experiments $np$ FSI effects must be quite significant even at the angles of $pp$ QFS. An independent approach viz. the $\frac{N_{ppn}}{N_{pp}}$ ratio gives consistent estimations of the QFS contributions to $pp$ coincidence spectra. This conclusion should be taken into account in the projects of experimental studies of $nn$ QFS. Apparently complete experiments are preferable because they allow to separate the process investigated from the background and to compensate additional expenses for obtaining the required statistics by a more reliable theoretical interpretation of the data. Somebody may say that PWIA and Watson–Migdal models are not applicable because multiple scattering effects are important. Nevertheless these models reproduce relative distributions of products in quite a satisfactory way even at much lower energies and have been successfully used up till now [19]. Actually, only relative distributions of products calculated are used to draw our conclusions.

I am grateful to the computer center staff for computer service and to my colleagues V. Pirnak and O. Povoroznyk for their help in calculations.

[1] H. Kumpf, in: *Proceedings of the VII International Conference on Few Body Problems in Nuclear and Particle Physics, Dehli, 1976* (Amsterdam, 1976), p. 225.
[2] B. Th. Leeman, M. G. Pugh, N. S. Chant, C. C. Chang, Phys. Rev. C **17**, 410 (1978).
[3] R. G. Allas, L. A. Beach, R. O. Bondelid, L. T. Myers, E. L. Petersen, J. M. Lambert, P. A. Treado, I. Šlaus, Nucl. Phys. A **304**, 461 (1978).
[4] L. A. Golovach, V. I. Grantcev, V. V. Zerkin, V. I. Konfederatenko, O. F. Nemets, R. G. Offengenden, O. M. Povoroznyk, B. A. Rudenko, V. A. Stepanenko, B. G. Struzhko, A. M. Shydlyk, Izv. Akad. Nauk USSR, Ser. Fiz. **51**, 166 (1987).
[5] N. Koori, T. Ohsawa, S. Seki, H. Yokota, T. Yanabu, Y. Deschamps, E. Hourani, H. Langevin–Joliot, F. Reide, M. Roy–Stephan, Phys. Rev. C **31**, 246 (1985).
[6] R. E. Warner, Phys. Rev. C **24**, 2759 (1981).
[7] B. Struzhko, Ukr. Phys. J. **43**, 305 (1999).
[8] R. E. Warner, S. B. Dicenzo, G. C. Ball, W. G. Davies, A. J. Ferguson, J. S. Forster, Nucl. Phys. A **243**, 189 (1975).
[9] Zhang Ying–Ji, Yang Jin–qing, Zhang Jie, He Jian–hua, Phys. Rev. C **45**, 528 (1992).
[10] Zhang Ying–Ji, He Jian–hua, Yang Jin–qing, Zhang Jie, Phys. Rev. C **47**, 468 (1993).
[11] V. I. Konfederatenko, Vit. M. Pirnak, V. A. Pylypchenko, O. M. Povoroznyk, B. G. Struzhko, H. Guratch, Ukr. Phys. J. **42**, 1175 (1997).
[12] M. Furic, H. H. Forster, Nucl. Instrum. Methods **98**, 301 (1972).
[13] I. Šlaus, R. G. Allas, L. A. Beach, R. O. Bondelid, E. L. Petersen, J. M. Lambert, P. A. Treado, R. A. Moyle, Nucl. Phys. A **286**, 67 (1977).
[14] G. Paič, J. C. Koung, O. J. Margaziotis, Phys. Lett. B **32**, 437 (1970).
[15] W. Kluge, Fortschr. Phys. **22**, 691 (1974).
[16] R. Machleidt, Adv. Nucl. Phys. **19**, 189 (1989).
[17] Ian H. Sloan, Phys. Rev. **185**, 1361 (1969).
[18] R. A. Cecil, B. D. Anderson, R. Madey, Nucl. Instrum. Methods **161**, 439 (1979).
[19] P. D. Felsher, C. R. Howell, W. Tornow *et al.*, Phys. Rev. C **56**, 38 (1997).

## ВЗАЄМОДІЯ В КІНЦЕВОМУ СТАНІ ТА КВАЗІВІЛЬНЕ РОЗСІЯННЯ В ЧОТИРИЧАСТИНКОВОМУ КАНАЛІ РЕАКЦІЇ $d+d$ ПРИ ЕНЕРҐІЇ 46.7 MeV

Б. Стружко
*Інститут ядерних досліджень НАН України*
*просп. Науки, 47, Київ–28, 03028, Україна*
*E–mail: struzh@marion.iop.kiev.ua*

Розраховано спектри збігу продуктів чотиричастинкового каналу реакції $d+d \longrightarrow p+p+n+n$: подвійного протон–протон ($pp$) і потрійного протон–протон–нейтрон ($ppn$). Теоретична модель враховує квазівільне розсіяння (КВР) $pp$ в імпульсному наближенні плоских хвиль та взаємодію в кінцевому стані обох пар нейтрон–протон в наближенні Ватсона–Міґдала. Результати узгоджуються з експериментальними даними, отриманими при енерґії пучка $E_0 = 46.7$ МеВ в кінематичних умовах КВР $pp$, яким відповідають кути емісії протонів в лабораторній системі $\vartheta_1 = \vartheta_2 = 38.75°$, $\varphi_1 - \varphi_2 = 180°$ та нейтрона $\vartheta_n = 0°$. Виявлено, що в спектрі подвійного збігу протонів переважає внесок послідовного процесу $d+d \longrightarrow d^*+d^* \longrightarrow p+p+n+n$ і лише біля чверті всіх подій можна віднести на рахунок квазівільного розсіяння. Цей висновок узгоджується також зі співвідношенням між кількістю подій потрійного й подвійного збігу в експериментальних та модельних спектрах.